

Modeling of Static Surface Error in End-Milling of Thin-Walled Geometries

Neha Arora, Ankit Agarwal, K. A. Desai*

Department of Mechanical Engineering, Indian Institute of Technology Jodhpur,
Jodhpur- 342037, Rajasthan, India

Abstract

In recent years, machining replaced metal working and assembly operations as a process to fabricate thin-walled components in the monolithic form. End Milling is preferred machining operation for such components due to its versatility to generate complex shapes in a variety of materials with high quality and productivity. End Milling is an intermittent cutting process with periodically varying cutting forces that causes deflection of thin-walled components owing to lower rigidity. The inherently low stiffness of thin-walled components introduces machining challenges related to static deflections of components. These deflections will result into significant amount of surface error and violation of machining tolerances. Therefore, prediction and control of surface error is an important task for process planners in achieving dimensional accuracy. This paper presents Finite Element Analysis (FEA) based methodology to predict static deflections of thin-walled components during end milling operation. The FEA model inputs cutting force values from two different variants of Mechanistic model existing in the literature and predicts static deflections. The values of deflections estimated from FEA model are transformed further into error profile using surface generation mechanism. An existing classification scheme has been modified to correlate cutting conditions and surface error profile. The results conceptualized based on surface generation mechanism are validated by performing computational experiments using commercial FEA package. The paper also investigates some of the important issues prevailing during machining of thin-walled components such as *thinning* and *end effects*.

Keywords: End Milling; Thin-Walled Component; Workpiece Deflection; Surface Error; FEA modeling

1. INTRODUCTION

End milling is a preferred manufacturing operation for Thin-walled components due to its versatility to generate complex shapes in a variety of materials with higher quality and productivity. In many cases, more than 90% of the material is removed from a block eliminating need for expensive multi-part manufacturing, large setup times on different machines and assembling of pieces together into finished product as a complete part is manufactured from the single component. Thin-walled components are extremely '*flexible*' owing to their lower rigidity and deflects easily under action of cutting forces. The relative position between tool and workpiece changes significantly due to deflections which results into surface errors on machined components. This necessitates development of reliable models which aids process planners in selection of optimum cutting conditions to obtain consistent part shapes with required accuracy. The present study achieves this objective by combining Finite Element Method (FEM) and machining mechanics using Mechanistic force model to predict workpiece deflections. The deflections are further transformed into surface error using surface generation mechanism.

Cutting force model is the fundamental element in milling process simulation as it helps in analyzing the process without conducting rigorous experimentation. A series of force models are reported in the literature which can be grouped into three categories; Experimental models [1,2], Mechanics based analytical force models [3,4] and Mechanistic force models [5,6,7 8]. The present study uses Mechanistic force model due to its ease of implementation and integration with other elements involved in predicting surface error [5]. Mechanistic force model simulates milling process into discrete increments; angle by angle, flute by flute and by dividing an end mill into axial segments slice by slice.

A similar model was developed by Desai and Rao [8] which has been used in this study to predict cutting forces. The static deflections of thin-walled component can be estimated using FEM and number of attempts are reported in the literature. Kline *et al.* [5] developed a computational methodology to predict cutter-workpiece deflections by applying concentrated force at force center. Tsai and Liao [9] recommended use of 12-node iso-parametric element to approximate tool-workpiece transient in an effective manner. Bera and Desai [10] extended application of FEM to predict deflections of thin-walled circular and tubular components. Once the nodal deflection values are obtained from FEM model, it has to be transformed into surface error using surface generation mechanism. This requires tracing of flute movement in the axial and feed direction. It has been reported in recent studies that the axial variation of tool deflection induced surface error can be linked with Axial Depth of Cut (ADOC) and Radial Depth of Cut (RDOC) and various error profiles were conceived on the basis of similarities in the flute engagement [11]. But, a similar study is not reported for thin-walled components yet where workpiece deflections are significant.

This paper extends existing classification scheme to the case of thin-walled machining and conceptualizes various error profiles. In machining of thin-walled structures, rigidity of the workpiece diminishes continuously from the start to end of the cut. Due to rigidity reduction of machined component, it gets thinner along the length which results into varying surface errors along feed direction. The effect of thinning and free ends of component is also highlighted in the paper. Henceforth, the paper is organized as follows; Section 2 present methodology for FEM of thin-walled components and translating deflection values into surface error. It also conceptualizes various surface error shapes based on classification scheme presented by Desai and Rao [11]. Section 3 presents computational results obtained using commercial FEM package along with *thinning* and *end effects*. The paper ends with summary of contributions from the present work in Section 4.

*Author to whom correspondence should be made, Email: kadesai@iitj.ac.in

2. PREDICTION OF SURFACE ERROR

The methodology to predict surface error requires systematic procedure determining cutting forces, deflection of thin-walled component and surface generation mechanism. The cutting forces are estimated based on Mechanistic force model developed by Desai and Rao [8] which provides cumulative cutting force at a given cutter rotation angle as well as discrete force values on engaged axial disc elements which can be input to FEM based workpiece deflection model. In the first case, the cumulative cutting force at a given cutter rotation angle is applied at the node corresponding to geometric center of the tool-workpiece transition area as depicted in Fig. 1. Meanwhile, distributed forces are applied along the line in the second case representing a flute oriented at helix angle (β) to the vertical edge of rectangle representing cutter-workpiece contact area. This requires meshing of transition area in a unique manner such that the aspect ratio of quad element is equal to $\tan \beta$ as shown in Fig. 1. The mesh is swept further along the plate thickness with relatively finer mesh in the transition region. The plate is modeled and analyzed as Free-Free-Free-Clamped (FFFC) state as shown in Fig. 1.

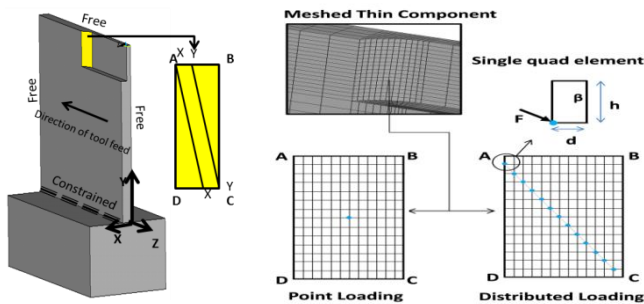


Figure 1: FEM of thin-walled component

The machined surface is generated in milling when a flute intersects workpiece surface or previous tooth trajectory. Depending upon geometry of the cut, a single or multiple flutes may be engaged into the cut with some axial nodes generating machined surface. Due to helix angle, axial location of surface generation point changes continuously with cutter rotation. The detailed procedure for tracing the flute movement and surface generation can be found from the previous literature [11]. The static deflection of a node in the direction normal to workpiece surface at the instant of surface generation has to be transformed into surface error. An automated routine has been developed in the present work which stores workpiece deflections determined from FEM at nodes corresponding to surface generation points. Simultaneously, it also stores axial location of surface generation point to derive surface error map in the axial and feed direction.

2.1. Classification of error profiles

It has been realized in previous studies that the magnitude of cutting force is dependent on tool material and geometry, workpiece material and geometry, cutting conditions etc., but the force profile is dependent on RDOC and ADOC only [12]. The change of RDOC and ADOC influences dimensions of rectangle ABCD in Fig. 1. Therefore, the change of RDOC and ADOC will result into change of engagement in radial direction (θ_{en}) and axial direction (θ_{sw}) respectively. Based on similarities in the engagement pattern, Desai and Rao [11] conceived various surface error profiles due to tool deflections. The study formulated five distinct relationships viz. $\theta_{en} + \theta_{sw} (\leq, \geq) \phi_p$; $\theta_{en} (\leq, \geq) \theta_{sw}$; $\theta_{en} (\leq, \geq) \phi_p$; $\theta_{sw} (\leq, \geq) \phi_p$; $\theta_{en} + \theta_{sw} (\leq, \geq) \phi_p$ to distinguish similarities of flute engagement and conceived six possible shapes of surface error termed as Type I-VI cutting. Here, ϕ_p is the pitch angle of

cutter. The same classification scheme has been extended in the study to thin-walled components where workpiece deflections dominate surface error profile. Type IV cutting representing combined up and down milling is not considered in the study to restrict scope of the present work to down milling.

2.1.1 Type I cutting ($\theta_{en} + \theta_{sw} \leq \phi_p$ and $\theta_{en} \geq \theta_{sw}$):

In this case, combination of ADOC and RDOC is such that the summation of θ_{en} and θ_{sw} is less than ϕ_p therefore, only single flute is engaged in the cut. The axial profile of surface error is completely dependent on forces experienced by engaged flute only. As flute engages into the cut, cutting force increases from D to A due to increase in chip load. As engagement angle is more than sweep angle, flute starts disengaging from vertex C after passing through A. In the meantime, chip load decreases due to reduction of engaged flute length. The resultant cutting force profile is shown in Fig. 2 (a). Although surface generation point traverses towards cantilevered portion of the plate, it deflects on the same lines as variation of cutting forces. The movement towards cantilevered portion does not have significant effect due to higher rigidity of the workpiece. Thus, maximum deflection is expected at the bottom of plate as cutting force is significantly higher. The deflection reduces to almost zero at the top of cut due to negligible cutting forces at that instant. The variation of surface error along axial length is depicted in Fig. 2(b).

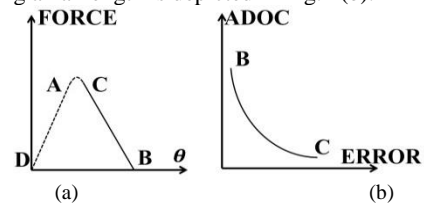


Figure 2: Type I Cutting (a) Force Profile; (b) Surface Error

2.1.2. Type II cutting ($\theta_{en} + \theta_{sw} \leq \phi_p$ and $\theta_{en} < \theta_{sw}$):

In this case, summation of θ_{en} and θ_{sw} is less than ϕ_p . But, θ_{sw} is more than θ_{en} therefore, the flute traverses through vertex C before A. As flute disengagement commences from C, it has definite chip load value which is invariant until A is traversed resulting into constant forces during this period. However beyond A, chip load decrease due to reduction in engaged flute length. The axial location corresponding to flute at A can be determined using formulation presented in Desai and Rao [11]. The variation of surface error beyond point A follows Type I cutting.

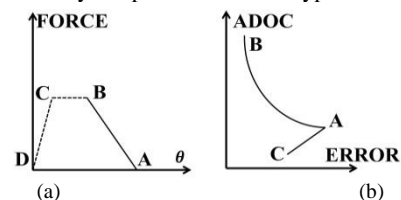


Figure 3: Type II Cutting (a) Force Profile; (b) Surface Error

2.1.3. Type III cutting ($\theta_{en} > \theta_{sw}$ and $\theta_{en} < \phi_p$):

The cutting conditions involving more than one flute engaged in the cut at a time are explored further. The summation of engagement angle and sweep angle is greater than the pitch angle for this case. As multiple flutes are engaged in the cut, the model generates force values for each disc corresponding to engaged flutes. These forces are applied on individual engaged disc element for distributed loading case to imitate the actual cutting condition. However in case of point loading, forces contributed by all in-cut flutes are summed and applied at the center of transition area.

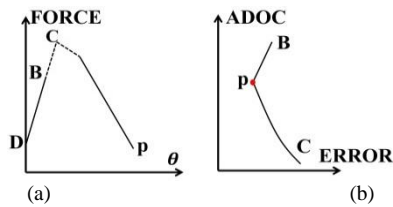


Figure 4: Type III Cutting (a) Force Profile; (b) Surface Error

Type III cutting configuration is such that the previous flute is generating machined surface when current flute enters the cut but it disengages before current flute engages fully. The axial location of previous flute at the time of entry of current flute is marked as **p** in Fig. 4(b) and its location can be found from Desai and Rao [11]. The surface error profile generated by previous tooth is resultant of combined cutting action of current and previous flute. The cutting forces increase during this period accompanied by surface generation point moving to more cantilevered portion resulting into increase of surface error which is shown as **pB** in Fig. 4(b). The machined surface from **C** to **p** is generated by the current flute which follows similar trend as Type I cutting.

2.1.4. Type V cutting ($\theta_{sw} > \theta_{en}$ and $\theta_{sw} < \phi_p$)

In this case, relationship between θ_{sw} , θ_{en} and ϕ_p is such that it represents combination of Type II and III cutting. The previous flute generates machined surface from point **p** to **B** in the same manner as Type III cutting. The current flute commences generating machine surface as it passes through vertex **C**. Since θ_{sw} is much higher than θ_{en} , vertex **C** is reached well before traversing through **A** (also designated as point **q**). The magnitude of chip load and cutting force is constant during flute movement from **C** to **A**. The deflection of thin-walled component is expected to increase from point **C** to **q** as surface generation point moves towards cantilevered portion with constant force. The axial location of previous flute at the time of entry of current flute (**p**) and the one corresponding to current flute passing vertex **A** (**q**) can be obtained based on discussions in Section 2.1.2 and 2.1.3. During flute movement from **A** to **p**, the chip load and cutting force decreases due to reduction of flute length. The reduction of surface error is observed between **q** and **p**. The resultant surface error profile for this case is schematically presented in Fig. 5(b).

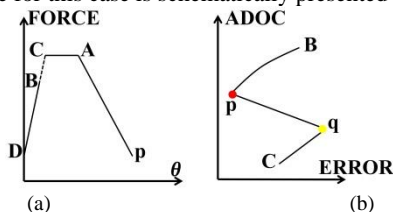


Figure 5: Type V Cutting (a) Force Profile; (b) Surface Error

2.1.5. Type VI cutting ($\theta_{sw} > \theta_{en}$ and $\theta_{sw} > \phi_p$)

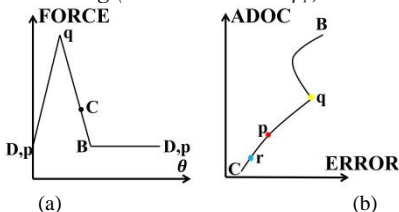


Figure 6: Type VI Cutting (a) Force Profile; (b) Surface Error

Type VI configuration represents combinations with higher ADOC values therefore, θ_{sw} is significantly higher than θ_{en} . As current flute enters in the cut, previous flute is generating machined surface at **p** and its axial location can be obtained in a similar manner as Type III cutting. The previous flute did not

traverse through **C** at this instant as ADOC is significantly higher. The chip load for previous flute is constant during this period however, chip load and cutting forces increases for current flute. Therefore, resultant surface error profile generated by previous flute is shown as **pq** in Fig. 6(b). In the meantime, current flute traverses through **C** and begins generating machined surface simultaneously with previous flute at different axial location. When current flute reaches axial location **r**, previous flute leaves the cut. During this period, the chip load experienced by current flute is constant. However, chip load on previous flute decreases resulting into segment **Cr** in the profile. Beyond axial location **r**, chip load and forces are invariant with flute generating segment **rp** in the profile. Beyond **q**, previous flute generates machined surface till current flute reaches **r**. Two opposing factors occur simultaneously during this period. The effective chip load and cutting forces decrease during this period but surface generation point traverses to deflection prone axial location from **q** to **B**. The balancing of these opposing factors result into segment **qB** in the error profile as shown in Fig. 6(b).

3. COMPUTATIONAL RESULTS

The classification scheme presented in previous section has been implemented in the form of a computational program to predict surface error variation in milling of thin-walled components. The cutting force values were obtained from Mechanistic force model developed by Desai and Rao [8] and workpiece deflection has been computed using FEA model developed using ANSYS APDL. The results are obtained using two different approaches discussed in the previous chapter; point loading at the center of cutter contact area and distributed loading on various nodes along helix. The computational experiments were conducted within end mill of four flutes, 30° helix angle and 16 mm diameter. The workpiece material was Aluminum 6061 with dimensions, 100mm x 50mm x 5mm. The subsequent subsections summarize results showing effect of loading, effect of ADOC and RDOC on error profile and thinning of thin-walled components due to material removal.

3.1 Effect of Loading

Mechanistic model predicts cutting forces with incremental rotation of the cutter either as a single cumulative value or acting on individual disc elements. If a simplified model or experimentally measured forces are used, a single value of cutting force is used in predicting workpiece deflections. Alternatively, it also provides nodal values of forces acting on each disc element which can also be used in predicting deflections. The present study uses both these models to predict workpiece deflections. The computational results are obtained at middle of the length of cut i.e. 50% material removed along feed direction.

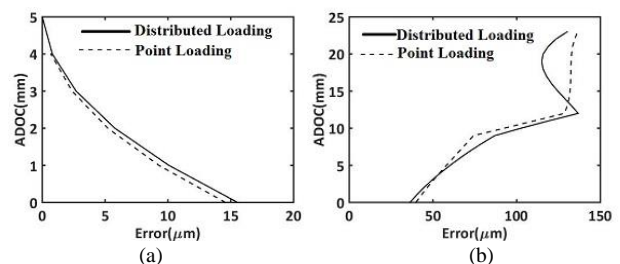


Figure 7: Surface Error profile for different Loading Conditions; (a) Type I Cutting (b) Type VI Cutting

Figure 7 shows comparison of error profile obtained from point and distributed loading approach for Type I and VI cutting. It can be seen from Fig. 7(a) that the predictions of both approaches are similar for cases with lower ADOC and RDOC values. Figure.

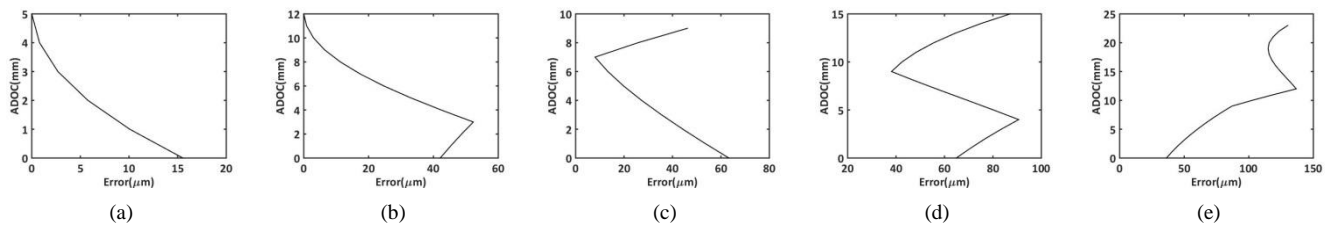


Figure 8: Surface Error Profiles in Various Cutting Zones

7(b) shows surface error variation for Type VI cutting representing aggressive cutting conditions in the form of higher ADOC and RDOC values. It can be seen that the application of point loading does not predict magnitude as well as shape of surface error accurately. This is due to simplified assumption in the form of single value of cutting force acting at middle of contact area. Therefore, distributed loading approach is used further in the study to substantiate the effect of ADOC and RDOC

3.2 Effect of ADOC and RDOC

In order to substantiate the effect of ADOC and RDOC on surface error profile, computational experiments were performed at different cutting conditions. These conditions were chosen such that each combination corresponds cutting types discussed in the previous section. The cutting conditions are summarized in Table 1. The computational results for various cutting types are shown in Fig. 8. It can be seen that the surface profile correspond well with the expected results discussed in the previous section. Table 1 presents comparison of axial location of various segments in the profile computed based on mathematical formulations presented by Desai and Rao [11] with its counterparts determined from computational experiments. Based on the results presented in Fig. 8 and Table 1, it can be inferred that the proposed classification scheme is quite effective in categorizing various surface error shapes.

Table 1: Cutting Conditions and Results

Type	ADOC (mm)	RDOC (mm)	Predicted Value (mm)	Computational Value (mm)
I	5	2	----	----
II	12	1.5	$Z_a = 3.37$	$Z_a = 3$
III	10	4	$Z_p = 7.26$	$Z_p = 7$
V	16	3	$Z_p = 9.36$ $Z_q = 3.59$	$Z_p = 9$ $Z_q = 4$
VI	24	3	$Z_r = 2.23$ $Z_p = 9.35$ $Z_q = 11.58$	$Z_r = 2$ $Z_p = 9$ $Z_q = 12$

3.3 Effect of Thinning

The rigidity of thin-walled components reduces significantly with the progress of machining resulting into increase of deflections and surface error. In order to investigate this aspect, computational experiments are conducted at five different locations i.e. 10%, 30%, 50%, 70% and 90% along length of the component. The error is computed at the top bottom and middle of axial depth of cut. It is anticipated that free ends are prone to significant deflections compared to center of the component. The free ends of component corresponding to start of the cut deflects more than the center of the plate. The other free end corresponding to end of cut has significantly higher surface error than the starting free end and middle of the component. This is due to significant reduction in rigidity of the

component with progress of machining which results into significant deflections and surface error towards end of the cut.

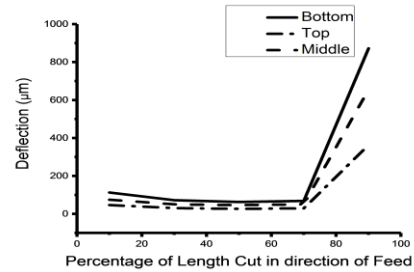


Figure 9: Surface Error Variation along Length of Cut

4. CONCLUSION

This paper presented an approach to predict axial variation of surface error during machining of thin-walled components. The approach uses cutting forces predicted using Mechanistic force model to determine static deflections. The forces were input to the computational program developed using commercial FEA package ANSYS APDL to estimate workpiece deflections. It is demonstrated that the distributed loading approach is computationally expensive but yields accurate results in comparison to point loading for thin-walled components. The deflections are transformed into surface error using surface generation mechanism. The paper conceptualizes various shapes of surface error profile for thin-walled components. The derived shapes are substantiated further by conducting series of computational experiments on thin-walled components. It has been concluded that the classification scheme developed in earlier studies for various error shapes can be extended to thin-walled components with minor modifications.

ACKNOWLEDGEMENT

The authors thank DST - Science and Engineering Research Board (SERB), Government of India for providing financial support to carry out the present research work.

References

- [1] J.J.J. Wang, S.Y. Liang, W.J. Book., Convolution analysis of milling force pulsation, Trans. of the ASME, Journal of Engineering for Industry, 116: 17–25, 1994.
- [2] T.S. Ong, B.K. Hinds, The application of tool deflection knowledge in process planning to meet geometric tolerances, International Journal of Machine tools and Manufacture 43: 731–737, 2003.
- [3] E.J.A. Armarego, N.P. Deshpande., Computerized end-milling force predictions with cutting models allowing for eccentricity and cutter deflections, Annals of the CIRP, 40: 25–29, 1991.

- [4] X.P. Li, A.Y.C. Nee, Y.S. Wong, and H.Q.Zheng, Theoretical modeling and simulation of milling forces. *Journal of Material Processing Technology*, 89–90: 266–272, 1999.
- [5] W.A. Kline, R.E. Devor, and I.A. Shareef., The Prediction of Surface Accuracy in End Milling. *Trans. ASME Journal of Engineering for Industry*, 104: 272-278, 1982.
- [6] W.S. Yun, D.W. Cho, K.F. Ehmann., Determination of constant 3D cutting force coefficients and of runout parameters in end milling, *Trans. of NAMRI/SME*, 27: 87–92, 1999.
- [7] M. Wan, W.H. Zhang, K.P. Qiu, T. Gao, Y.H. Yang., Numerical prediction of static form errors in peripheral milling of thin-walled workpieces with irregular meshes, *Trans. of the ASME: Journal of Manufacturing Science and Engineering*, 127: 13-22, 2005
- [8] K.A. Desai, P.V.M. Rao., Process geometry modeling with cutter runout for milling of curved surfaces, *International Journal of Machine Tools and Manufacture*, 49:1015-1028, 2009.
- [9] J.S. Tsai, C.L. Liao, Finite-element modeling of static surface errors in the peripheral milling of thin-walled workpiece, *Journal of Material Processing Technology*, 94: 235–246, 1999.
- [10] T.C. Bera, K. A. Desai, On milling of thin-walled tubular geometries, *Proceedings of the Institution of Mechanical Engineers, Part B: Journal of Engineering Manufacture*, 224: 1804-1816, 2010.
- [11] K.A. Desai, P.V.M. Rao., On cutter deflection surface errors in peripheral milling, *Journal of Materials Processing Technology*, 212: 2443-2454, 2012.
- [12] L. Yang, R.E. DeVor, S.G. Kapoor, Analysis of force shape characteristics and detection of depth-of-cut variations in end milling, *Trans. of the ASME: Journal of Manufacturing Science and Engineering*, 127: 454–462, 2005.